Int. J. Solids Structures Vol. 30, No. 3, pp. 359–370, 1993
Printed in Great Britain.

0020–7683/93 $5.00+ .00

GLOBAL INSTABILITY AND BIFURCATION IN BEAMS COMPOSED OF ROCK-LIKE MATERIALS

L. BIOLZI† and J. F. LABUZ
Department of Civil and Mineral Engineering, University of Minnesota, Minneapolis, MN 55455-0220, U.S.A.

(*Received* 18 *November* 1991; *in revised form* 16 *July* 1992)

Abstract—The behavior of strain-softening structures in relation to their overall load-displacement response is examined as a stability problem of the global system. The prototype structure studied is the simple beam under three, four and five-point bend. It is demonstrated that fracture problems do not require geometric or material nonlinearity to produce instability—the size and shape of a structure that fails by fracture are the important factors that control the system. In addition, some geometries, for example the four and five-point-bend beams, may develop different crack configurations such that a bifurcation in the global equilibrium of the structure is possible. Experiments and analyses indicate that size, slenderness, constraint and symmetry of the deformed beam must be considered in predicting the post-failure response.

1. INTRODUCTION

As is now well documented by test results (Wawersik and Fairhurst, 1970; Bažant, 1976; Vardoulakis, 1980), strain softening is a characteristic displayed in several materials such as rock, concrete and dense soil. Softening is usually associated with a zone of localized deformation; inside the zone a decrease in stress is accompanied by an increase in strain, while outside the zone the strain decreases (Labuz *et al.*, 1985). When softening is involved with a structural component, a snap-back "instability" may occur, with the post-failure response taking on a positive slope (Berry, 1960; Cook, 1965; Maier, 1968; Bažant, 1976; Schreyer and Chen, 1986).

Usually, the stability of a mechanical system is connected with a monotonous load-displacement response; in this sense, softening is always associated with instability. For a softening structure, however, it is possible to observe

(a) stable softening or simply "stability", if the load-displacement response in the post-peak regime is always characterized by a negative slope [Fig. 1(a)];

(b) unstable softening or simply "instability", if the softening branch takes on, at least in part, a positive slope [Fig. 1(b)].

The critical situation, which is the separation threshold between stability and instability, corresponds to a reduction of the load-carrying capacity at constant displacement [Fig. 1(c)].

One of the first attempts to incorporate softening behavior into an analysis of a beam was Wood's paradox (Wood and Roberts, 1966; Wood, 1968). Basically, Wood showed that one could not explain within a classical formulation how strain softening could spread from the midspan point into a segment of finite length. Inspired by this work, Maier (1968) proposed to describe the elastic behavior in terms of a local generalized-strain variable—

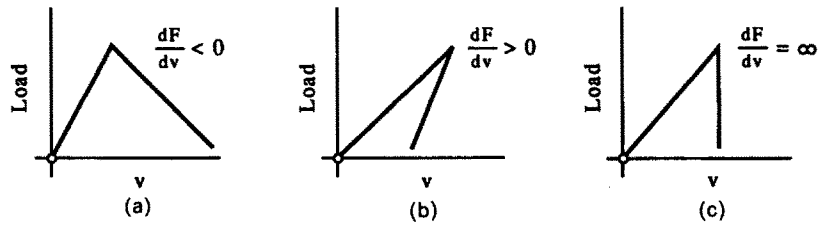

Fig. 1. Global response of elastic-softening structures: (a) stable; (b) unstable; and (c) critical.

† Present address: Dipartimento di Ingegneria Strutturale, Pol. di Milano, Italy.

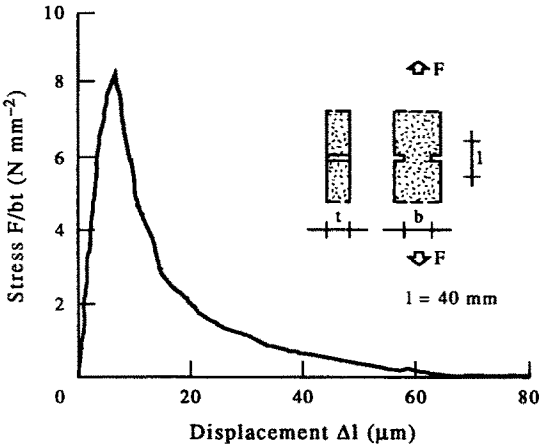

Fig. 2. Uniaxial tensile test on granite.

the curvature—and the softening behavior in terms of a nonlocal generalized—strain variable—the rotation of a plastic hinge. Later, Bažant (1976) pointed out that a local constitutive theory inevitably leads to a softening zone of negligible thickness and zero energy dissipation, whereas neither feature is supported by experimental evidence. Ottosen (1986), on the basis of a thermodynamic consideration for a simple unidirectional problem, proved that the width of the localization zone must decrease to zero, thereby violating the classical definition of strain.

To predict a softening zone of finite thickness, a nonlocal constitutive equation must be postulated (Schreyer, 1990). One such approach is through the introduction of ideas typical in fracture mechanics, namely, fracture energy and a characteristic length. For instance, an elastic–plastic constitutive law can be adopted for the local strain components, while the softening behavior can be described in terms of a stress–crack opening relation (Hillerborg *et al.*, 1976; Bažant and Chang, 1987; Carpinteri, 1989).

Shown in Fig. 2 is a typical result from three tensile tests performed on a softening material—granite—using the double-edge-notched specimen under displacement control. In uniaxial tests on rock, the deformation begins to localize in the hardening regime, and the stress field becomes a combination of pure tension and bending. Nonetheless, the post-peak displacements are attributed to an average crack opening, such that the constitutive relation of the localized-fracture zone is given by the post-peak response (Labuz *et al.*, 1985).

The objective of this work is to demonstrate that fracture problems do not require geometric or material nonlinearity to produce instability—the size and shape of a structure that fails by fracture are the important factors that control the system. Closed-loop tests were conducted to record the global response of strain-softening beams. The experiments were analysed by considering the displacements in the elastic and inelastic (fracture) states. In particular, it will be shown that to study the problem of beams in flexure when the slenderness is varied, it is fundamental to consider the two-dimensional effects of load diffusion at the load points and reactions. Furthermore, size, constraint and symmetry of the deformed structure pose additional effects that have yet to be experimentally investigated. Although experiments and analyses were conducted on beams, the conclusions are general in a sense that all structures which soften due to crack growth exhibit "brittleness".

2. EXPERIMENTAL APPARATUS

The phenomenon of strain softening can be studied in the laboratory only within a closed-loop system (Fig. 3), where the feedback signal is adjusted to coincide with the desired program independent of the specimen and machine. Conventional load-prescribed testing machines cannot be used to capture the post-peak response. For this reason the notion of "brittle" behavior is sometimes associated with strain-softening materials, as

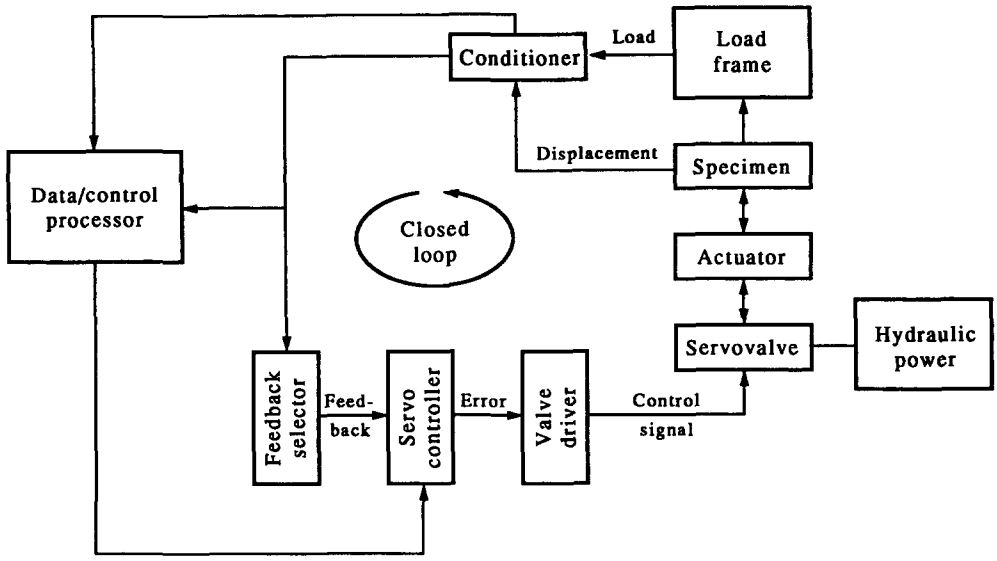

Fig. 3. Closed-loop testing system.

complete load-carrying capacity is lost after reaching maximum load in a dead-load system (Glucklich and Cohen, 1967; Hudson *et al.*, 1972).

With a displacement-controlled or "hard" device, it is possible to follow the softening response, regardless of machine stiffness, if the feedback signal is a monotonously increasing function with time (Hudson *et al.*, 1972; Cangiano and Tognon, 1990). The displacement that satisfies this condition for a bend test is due to crack opening and not the deflection of the load point, which can be affected by the energy stored in the structure and machine.

The influence of machine stiffness (Salamon, 1970; Cooper, 1977; Sture and Ko, 1978) on the post-peak response as measured by the load-point displacement can be illustrated by considering a rotation of the load axis, such that a stable response may show up as an instability (Fig. 4). The actual behavior is masked by an added contribution from the machine. This effect, as well as crushing at the contacts, can be eliminted by the measurement of a displacement relative to points directly above the supports (Bush, 1976). Note that a snap-back instability can still appear within an infinitely stiff machine when considering the load-point displacement.

Closed-loop fracture experiments were conducted in a 1 MN load frame using the displacement across a sawn notch as the feedback signal. A strain-gage based transducer monitored this so-called crack mouth opening displacement, which was programmed to increase at a rate of 2×10^{-4} mm s^{-1}. Two linear variable differential transformers, LVDTs

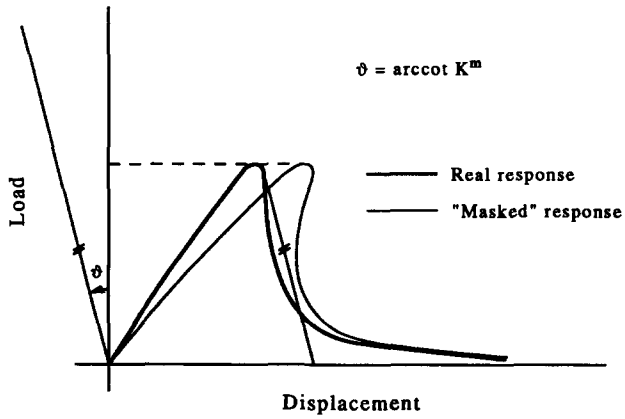

Fig. 4. Actual behavior and system behavior (machine and specimen); K^m is machine stiffness.

Table 1. Mechanical properties of the granite

σ_t[MPa]	E [GPa]	ν	G_f [kN m^{-1}]
8.2	31	0.24	0.24

with a linear range of 2.5 mm, were fastened symmetrically in the centerline of the beam to measure the (differential) load-point displacement. Test control and data acquisition were provided by a microcomputer. The specimen geometries were beams in three-point bending with simple support and with one redundant support (a five-point-bend test), and in four-point bending with symmetric and nonsymmetric crack configurations. At least three tests were performed for each condition.

The typical behavior of the material (granite) is illustrated in Fig. 2, and the mechanical properties are reported in Table 1. The elastic constants were evaluated by the active seismic technique with a *P*-wave analyser. The fracture energy was calculated from the uniaxial tensile tests (Fig. 2), whereas that provided by the classical three-point-bend configuration was larger. This probably is attributable to the additional energy dissipated by micro-cracking and crushing, which in a bend test, may produce a strong dependence on the specimen size and notch depth (Tognon and Cangiano, 1989).

3. INSTABILITY

To consider the instability of softening systems, experiments were performed with the three-point-bend configuration, a simple geometry characterized by a well-defined crack path. The behavior for beams of a given cross-section (50 mm height and 50 mm thickness) but different lengths is illustrated in Fig. 5. The global response ranges from instability for the short span, to stability, and back to instability for the slender beam. Consequently, the softening behavior that can be observed in an elastic-softening structure is not an essential material property, but rather a structural response.

Figure 6 shows the behavior of specimens that are geometrically similar. The beams exhibit a qualitative behavior evidently different: softening with an increase in displacement associated with a decrease in applied load for the smaller specimen (a stable condition) and a more brittle response in the larger specimen (an unstable condition). This is a manifestation of the so-called size effect, a factor of fundamental importance when laboratory experiments, carried out on small elements, are extrapolated to real structures of considerable size (Bažant, 1984).

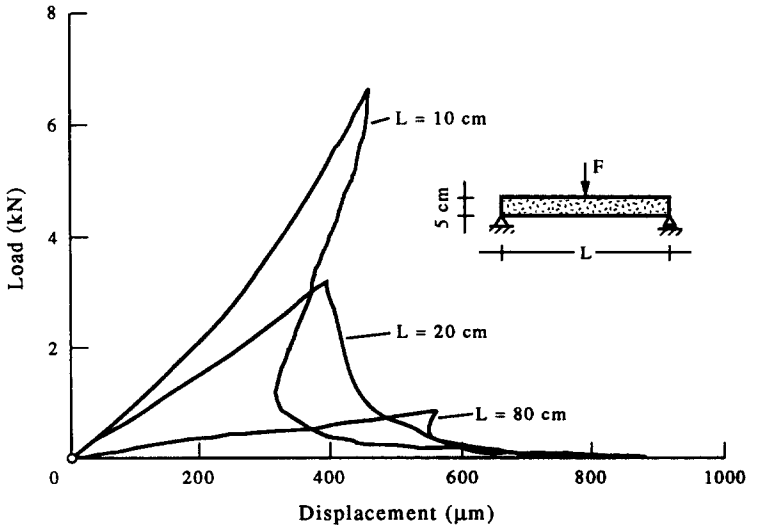

Fig. 5. Global response of short, intermediate, and long span beams of the same height.

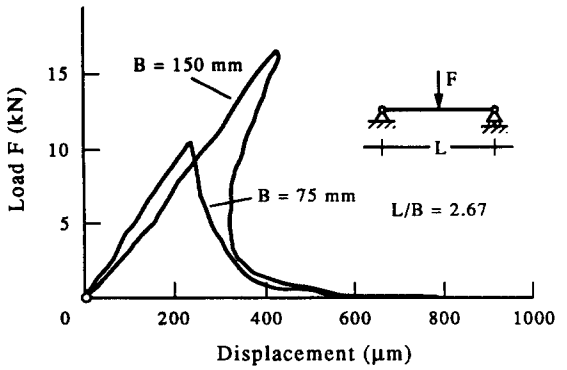

Fig. 6. Global response of two geometrically similar beams of different sizes.

The stability of the three-point-bend configuration may be analysed by considering the total displacement at the load-point application. The results that will be obtained for this beam hold for nonredundant beams with different constraints (for example, a cantilever beam). In addition, the present analysis can be applied to other geometries such as a beam in four-point bending, which will be considered later.

The total displacement v^t in a generic loading step is due to elastic v^e and inelastic (fracture) v^f displacements from the beam and possibly a component due to the machine v^m:

$$v^t = v^e + v^f + v^m. \tag{1}$$

If F is the load applied to the beam by the testing machine, the elastic part may be represented by

$$v^e = F\{L^3/(48EI) + \kappa L(1+\nu)/(2EBT) + [5/(ET) + 0.2L/(EBT)]\}, \tag{2}$$

where E is Young's modulus, ν is Poisson's ratio, κ is the form factor, L is the length, B is the height, T is the thickness, and I is the moment of inertia. The third term is due to the diffusive nature of the point loads and is a good approximation if the length of the beam is greater than $2B$ (Dischinger, 1932); a similar expression is reported in Timoshenko and Goodier (1970). With K^m denoting the machine stiffness per specimen thickness, the last term in (1) is

$$v^m = FT/K^m. \tag{3}$$

The inelastic part is due to the formation of a fracture zone, which is assumed to be fully developed at the peak load. Several observations reinforce the validity of this simplifying assumption: (1) Fig. 7(a) shows the strain at the midspan measured during a three-point-bend test at peak load; the strain distribution is strongly nonlinear, suggesting the existence of a stress concentrator. (2) A fracture strain of 300×10^{-6} has been recorded from uniaxial tension tests, so that the values of strain from the beam indicate that a fracture zone is

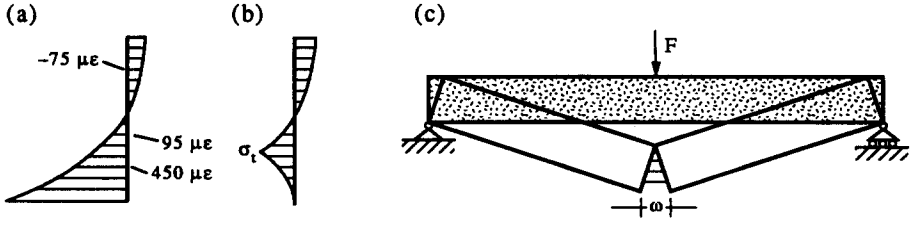

Fig. 7. (a) Measured-strain distribution; (b) hypothesized stresses; and (c) limit situation.

already present. (3) Localization is observed optically before peak load. Based on the measured strain data, the stress distribution is hypothesized to be that shown in Fig. 7(b).

A further idealization is to model the fracture as a cohesive zone (Dugdale, 1960; Barenblatt, 1962; Palmer and Rice, 1973), with a first order approximation of the closing stress being described by a linear function:

$$\sigma = \sigma_t(1-\omega/\omega_c). \tag{4}$$

Obviously, the cohesive-zone representation of the fracture process is not limited to rock-like materials, but can be applied to metals where the plasticity is confined to the crack plane.

From geometrical considerations, the displacement v^f can be written as

$$v^f = [G_f LB/(2\sigma_t)][1-\sigma/\sigma_t], \tag{5a}$$

if the crack opening ω in the lower part of the beam is less than or equal to the critical opening ω_c, and

$$v^f = G_f Lx/(2\sigma_t), \tag{5b}$$

if the crack opening is greater than the critical opening ω_c; x is the depth of the cohesive zone, and from (4), the fracture energy per unit crack extension is $G_f = \sigma_t\omega_c/2$.

At the limit load, the fracture zone is approximated as being distributed over the full height of the beam [Fig. 7(c)]. If instead of the load the stress from elementary beam theory is introduced, (1) may be written

$$v^t = [\sigma B/E][\lambda^2/6+\kappa(1+\nu)/3+2(5+0.2\lambda)/(3\lambda)+2TE/(3\lambda K^m)-G_f E\lambda/(2\sigma_t^2 B)], \tag{6}$$

where $\lambda = L/B$ is the slenderness of the beam. The incremental stability condition for critical softening is

$$dv^t/d\sigma = 0, \tag{7}$$

so (6) then reduces to

$$f(\lambda) = G_f E/(\sigma_t^2 B), \tag{8}$$

where $f(\lambda) = \lambda/3+2\kappa(1+\nu)/(3\lambda)+[4(5+0.2\lambda)/3+4TE/(3K^m)]/\lambda^2$. A different "global" stability criterion may be derived by comparing the total elastic energy stored in the beam and the machine with the fracture energy dissipated in the cohesive zone. In this case, we get a stability condition that is four times more restrictive in that an incremental snap-back may appear, but globally it would not be predicted (Labuz and Biolzi, 1991).

The right-hand side of (8) is sometimes referred to as a brittleness number (Cherepanov, 1979), and in some sense plays the same role as slenderness in elastic stability theory. For a given material with constant properties, a size dependence appears through the height (B) scale, which means that an instability would be observed when the specimen is above a critical size, as illustrated by the experiments (Fig. 6). This is a natural consequence of the mismatch in the elastic energy stored per unit of volume and the fracture energy dissipated per unit of area (Palmer and Rice, 1973), and holds for any type of elastic-softening fracture system.

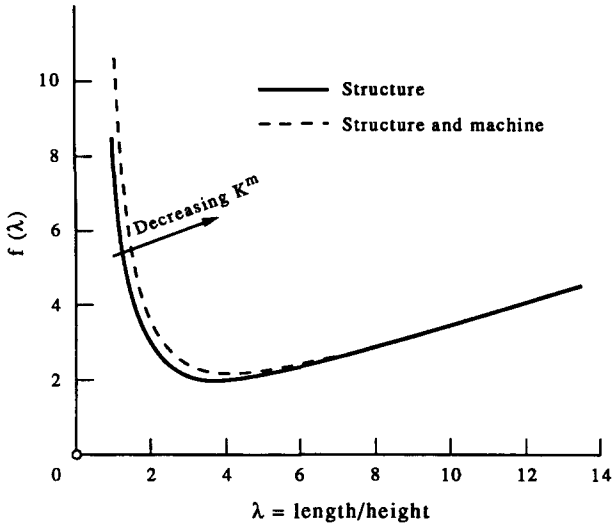

Fig. 8. Slenderness function $f(\lambda)$.

In addition to the size scale (for a given load configuration), the post-peak response is governed by the geometry, or in the case of a beam, the slenderness. Figure 8, a plot of the function $f(\lambda)$ assuming a Poisson's ratio of 0.24, reveals that a beam has two values of slenderness ($2.5 < \lambda < 6$) between which the load-displacement response is stable. Experiments (Fig. 5) confirm that for both high and low slenderness, the beam behaves in an unstable manner. This result is general and holds for all nonredundant beams with various constraints. Therefore, if the solutions to (8) are real, two values of slenderness define the stable range of the softening response for a given geometry and load configuration.

The influence of machine stiffness is also shown in Fig. 8. For a stiff (100 MN m^{-1}) load frame, the stability is affected only for beams of low slenderness ($\lambda < 6$). As the stiffness of the testing machine is reduced, the critical curve is shifted up and to the right, such that the post-peak response of a stubby beam becomes influenced by the machine. Consequently, if the measurement of the load-point displacement includes the deformation of the load frame, a system instability may be displayed (Fig. 4) when in fact the response of the beam is stable.

4. BIFURCATION

In the three-point-bend configuration, the crack pattern is well defined. This is not true, however, if a four-point-bend specimen (Fig. 9) where, due to loading and geometric

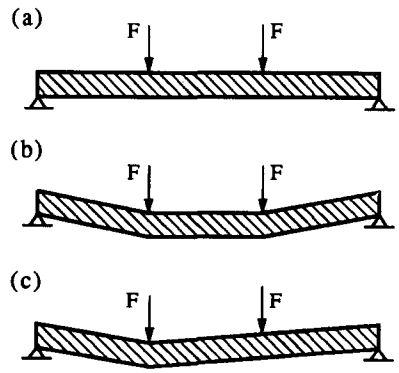

Fig. 9. (a) Four-point-bend beam; (b) symmetric; and (c) nonsymmetric failure modes.

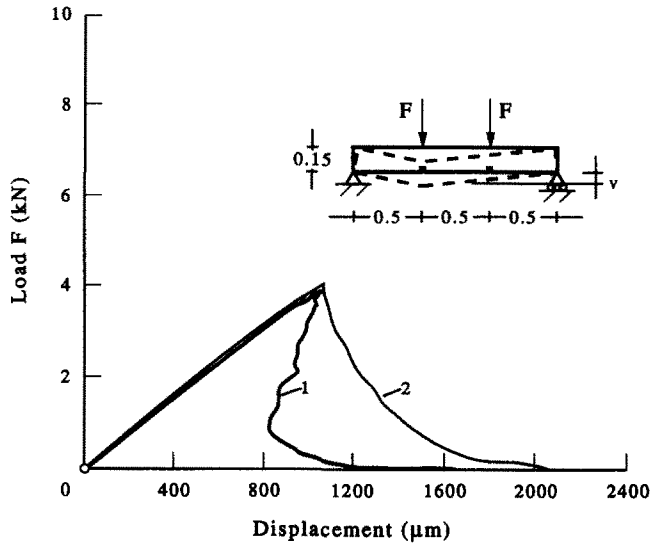

Fig. 10. Global response of the nonsymmetric (1) and symmetric (2) four-point-bend beams.

symmetry, we may have two cracks contributing to the system response. The post-peak behavior will be governed by whether the beam collapses in a symmetric or nonsymmetric manner. So, when the structure presents the possibility of two or more cracks developing simultaneously, a bifurcation of the load path in the softening regime may occur.

Figure 10 illustrates the load-displacement behavior recorded for a four-point-bend geometry in the nonsymmetric (curve 1) and symmetric modes (curve 2). In the first case, for the beam with a crack below only one of the load points, the failure process does not demand additional external work; the energy stored in the elastic phase of the beam is more than sufficient to drive the fracture. Conversely, with a symmetric cracked configuration, it is necessary to supply the fracturing process with additional work. Therefore, the four-point-bend beam may fracture in a nonsymmetric mode with the necessity of extracting energy from the structure, while in the symmetric case the system requires an input of energy to cause failure.

In order to predict the actual response, the second-order work must be examined (Maier *et al.*, 1973; Nemat-Nasser *et al.*, 1980; Bažant, 1989). If δF denotes the variation of the load associated with a small incremental displacement δv, the stable path that starts at a bifurcation point is characterized by the condition that the second-order work $\delta^2 W$,

$$\delta^2 W = 0.5(\delta F)(\delta v), \tag{9}$$

is a minimum.

For a comparison among two or more possible situations, it is convenient to write $\delta^2 W$ introducing the so-called tangent stiffness:

$$k_t = (\delta F)/(\delta v). \tag{10}$$

In this way (9) can be written

$$\delta^2 W = 0.5 k_t (\delta v)^2. \tag{11}$$

Alternatively, the second-order complementary work $\delta^2 W^*$ can be used:

$$\delta^2 W^* = 0.5 (\delta F)^2 / k_t, \tag{12}$$

and the actual response is characterized by its maximum value (Bažant, 1989).

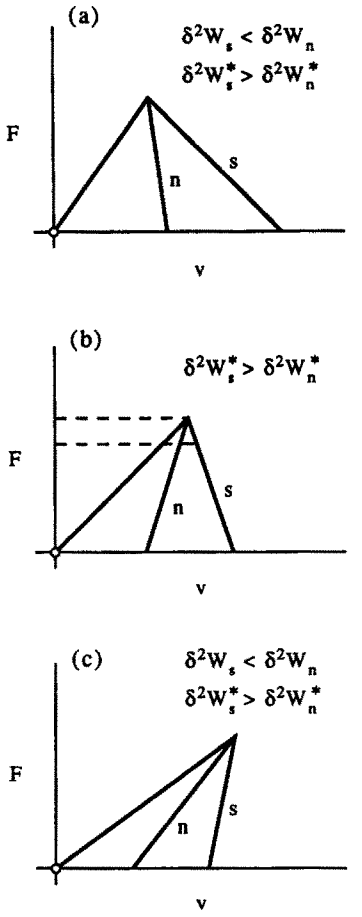

Fig. 11. Schematic representation of experimental results from four-point-bend tests.

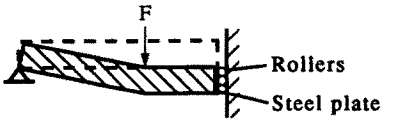

Fig. 12. Experimental scheme to enforce a symmetric failure mode in the four-point-bend beam.

Figure 11 is a schematic of three different cases that have been recorded experimentally. By considering (9) or (12), it can be verified that the nonsymmetric response is the preferred one, as is recorded in the tests. For example, Fig. 11(b) depicts the situation observed in the four-point-bend tests (Fig. 10). Referring to (12), we see that for the same variation the maximum value of $\delta^2 W^*$ is governed by the tangent stiffness k_t. For the nonsymmetric case k_t is positive, whereas k_t is negative in the symmetric failure mode. Similar arguments can be applied to Figs 11(a) and 11(c).

The actual post-peak behavior of the structures illustrated in Fig. 10 is characterized by one crack only. The symmetric crack configuration is experimentally impossible to obtain with conventional apparatus. It can be simulated, however, through an experimental stratagem (Fig. 12) by considering one half of the structure, such that symmetry of the displacements is enforced, even into the post-peak region. This problem has been analysed by Chen and Maier (1992).

5. DISCUSSION

The stability analysis already presented can be repeated for the nonsymmetric, four-point-bend configuration (4PB), with the following result:

$$f^{4PB}(\lambda) = G_f E/(\sigma_t^2 B), \tag{13}$$

where $f^{4PB}(\lambda) = 5\lambda/9 + \kappa(1+\nu)/\lambda + [(8.84+0.3\lambda)+4TE/(3K^m)]/\lambda^2$. If the left-hand side of (13) is compared with the analogous relation (8) for the three-point-bend (3PB) geometry, then for every λ one finds $f^{4PB}(\lambda) > f(\lambda)$. Thus, the set of slenderness values for stable softening is larger in a 3PB specimen, making it more stable. This is a direct consequence of the greater capacity of the 4PB beam to store elastic energy before collapse; for example, the displacements at the peak load for the 4PB specimen (Fig. 10) are larger than that for the 3PB (Fig. 5). However, the most stable configuration (for a given height) out of the 3PB, nonsymmetric 4PB, and symmetric 4PB is the latter because it dissipates twice the fracture energy. Experiments confirm this assertion, even though two cracks do not appear in an actual 4PB test.

Equation (8) or (13) may be solved for the height B to demonstrate that for a given structural geometry composed of a rock-like material, there exists a critical size-scale characterized by perfectly brittle behavior [Fig. 1(c)]. In this case, relatively small displacement increments correspond to a drastic decrease in load-carrying capacity. Physically, the critical condition is that for which all the potential elastic energy supplied to the beam in the loading phase is dissipated in the fracture process. The displacement due to elastic deformation along the beam is transformed into inelastic opening within the localized crack. Furthermore, for a given load configuration, a critical value of the brittleness number $G_f E/(\sigma_t^2 B)$ appears for which it is possible to observe a snap-back instability only, whatever the slenderness of the structure.

The next level of complication in terms of the simple beam is to provide a single degree of redundancy [Fig. 13(a)]. Again, an experimental stratagem to replicate this condition, in terms of the first instability, is to use a five-point-bend (5PB) beam loaded in the middle of the two spans [Fig. 13(b)]. The 3PB beam with one redundant support and the 5PB beam are not equivalent, however, in terms of the total system response. A nonsymmetric crack configuration will appear in the 5PB beam, as predicted by the minimum value of the second-order work $\delta^2 W$.

The results from these tests are shown in Fig. 14. We can observe that the beams with "one redundant support", that is the 5PB beams, showed two softening branches—the first due to fracture at the middle support (the fixed end) and the second caused by crack initiation below only one of the load points. The addition of one constraint produces the structural response with an additional softening branch. Furthermore, a structure with n-redundant constraints will exhibit at most $n+1$ softening branches, as suggested by Bažant *et al.* (1987) and recorded by Biolzi and Labuz (1989). Some of them, as in the case of structures with geometric and loading symmetries, theoretically may overlap each other, but material or geometric imperfections will prevent this.

For the tested load configuration, the 5PB beam, the first softening branch is due to the cracking of the upper portion at the central support. A bifurcation develops at the peak

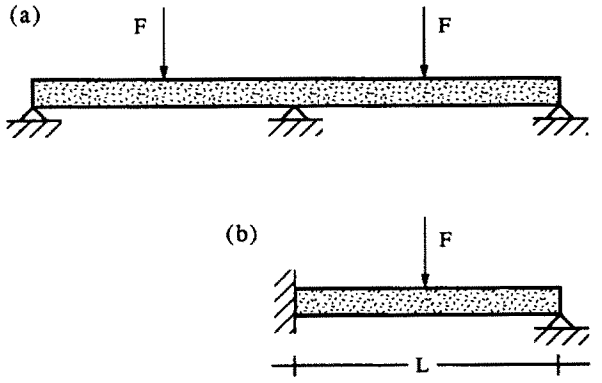

Fig. 13. Redundant systems.

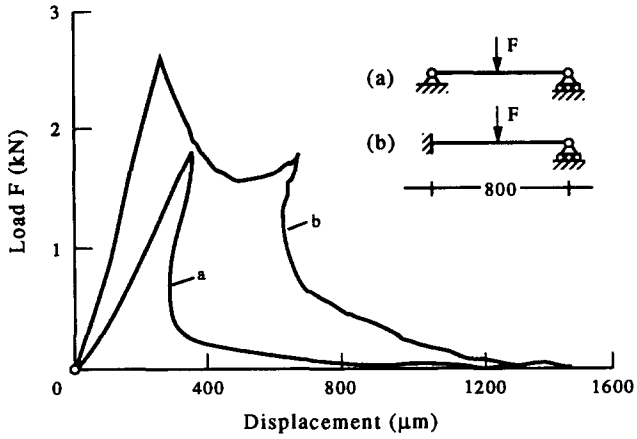

Fig. 14. Global response of three-point-bend beams with simple support (a) and one redundant support (b).

of the second softening branch, because one or two cracks are possible in the lower fiber below the load points. Experiments and $\delta^2 W$ suggest that only one crack will appear, so that the equivalence between the simple beam with one fixed end and the continuous beam is lost. If we consider a load configuration for the 5PB beam that produces the first crack below one of the external loads, the bifurcation point is shifted to the first peak load. The nonsymmetry of the deformed structure is then apparent within the first post-peak region.

6. CONCLUSIONS

The qualitative behavior of various beams was examined through a nonlinear model that considers the cohesive interaction of the fracture. Experiments support the use of a cohesive-zone representation, because for this material (granite), the main energy sink is due to the localized process zone within the main crack. Fracture tests and analyses suggest that it is not possible to define a structural brittleness in flexure without considering the influence of slenderness and load geometry; in fact, two values of slendeness define the stable range of softening. Machine stiffness may mask the global response of the specimen. This effect can be eliminated by using a differential measure of the load-point displacement, although a closed-loop system with the proper feedback signal is still needed to capture the instability; then, machine stiffness is not important.

For systems that fail due to crack propagation, the instability in the load-displacement response is a function of the size and shape of the structure, together with the mechanical properties of the material. When it is possible to have different crack configurations of the structure, a bifurcation of the global equilibrium may appear. Both experiments and the minimum value of the second-order work suggest that for the four and five-point-bend tests, the nonsymmetric failure mode is preferred.

In summary, fracture as a stability problem has an analogy with classical elastic stability. Both are characterized by instability and bifurcation phenomena, as well as nondimensional parameters—slenderness and brittleness.

Acknowledgements—Partial support from the National Science Foundation, grant number MSS-9109416 (program director K. P. Chong) and the Italian MURST is gratefully acknowledged. Special thanks are due to MTS Systems Incorporated (Minneapolis, Minnesota) and S. L. Crouch for providing the opportunity for L. Biolzi to visit the Department of Civil & Mineral Engineering of the University of Minnesota in Fall 1991 through the MTS Geomechanics Chair.

REFERENCES

Barenblatt, G. I. (1962). The mathematical theory of equilibrium cracks in brittle fracture. *Adv. Appl. Mech.* **7**, 55–129.

Bažant, Z. P. (1976). Instability, ductility and size effect in strain softening concrete. *J. Engng Mech. ASCE* **102,** 331–344.
Bažant, Z. P. (1984). Size effect in blunt fracture: concrete, rock, metal. *J. Engng Mech. ASCE* **110,** 518–535.
Bažant, Z. P. (1989). Stable states and stable paths of propagation of damage zones and interactive fractures. In *Cracking and Damage* (Edited by J. Mazars and Z. P. Bažant) pp. 183–206. Elsevier, Amsterdam.
Bažant, Z. P. and Chang, T. P. (1987). Nonlocal finite element analysis of strain softening solids. *J. Engng Mech. ASCE* **113,** 89–105.
Bažant, Z. P., Pijaudier-Cabot, G. and Pan, J. (1987). Ductility, snapback, size effect, and redistribution in softening beams or frames. *J. Struct. Div. ASCE* **113**(12), 2348–2364.
Berry, J. P. (1960). Some kinetic considerations of the Griffith criterion for fracture—1. Equations of motion at constant force. *J. Mech. Phys. Solids* **8,** 194–206.
Biolzi, L. and Labuz, J. F. (1989). Structural behavior of strain-softening beams. *Proc. Int. Conf. Recent Developments in Fracture of Concrete and Rock*, Cardiff, U.K. pp. 693–700. Elsevier, London.
Bush, A. J. (1976). Experimentally determined stress-intensity factors for single-edge-crack round bars loaded in bending. *Exp. Mech.* 249–257.
Cangiano, S. and Tognon, G. (1990). The ductile/brittle transition in concrete beams in relation to servo-controlled system of the testing machine. *Engng Fract. Mech.* **35**(4/5), 793–799.
Carpinteri, A. (1989). Decrease of apparent tensile and bending strength with specimen size: two different explanations based on fracture mechanics. *Int. J. Solids Structures* **25,** 407–429.
Chen, Z. and Maier, G. (1992). Bifurcation and instability in fracture mechanics of cohesive-softening media by boundary elements. *Fatigue Fract. Engng Mater. Struct.* (in press).
Cherepanov, G. P. (1979). *Mechanics of Brittle Fracture*. McGraw-Hill, New York.
Cook, N. G. W. (1965). The failure of rock. *Int. J. Rock Mech. Min. Sci.* **2,** 389–402.
Cooper, G. A. (1977). Optimization of the three-point bend test for fracture energy measurement. *J. Mat. Sci.* **12**(1), 277–289.
Dischinger, F. (1932). Beitrag zur theorie der halbscheibe und des wandartingen balkens. *I.V.B.H. Erster Band*, 63–93.
Dugdale, D. S. (1960). Yielding of steel sheets containing slits. *J. Mech. Phys. Solids* **8,** 100–104.
Glucklich, J. and Cohen, L. J. (1967). Size as a factor in the brittle–ductile transition and the strength of some materials. *Int. J. Fract. Mech.* **3,** 278–289.
Hillerborg, A., Modeer, M. and Petersson, P. E. (1976). Analysis of crack formation and crack growth in concrete by means of fracture mechanics and finite elements. *Cement Concrete Res.* **6,** 773–787.
Hudson, J. A., Crouch, S. L. and Fairhurst, C. (1972). Soft, stiff and servo-controlled testing machines: a review with reference to rock failure. *Engng Geol.* **6,** 155–189.
Labuz, J. F. and Biolzi, L. (1991). Class I vs Class II stability: a demonstration of size effect. *Int. J. Rock Mech. Min. Sci. Geomech. Abstr.* **28**(2/3), 199–205.
Labuz, J. F., Shah, S. P. and Dowding, C. H. (1985). Experimental analysis of crack propagation in granite. *Int. J. Rock Mech. Min. Sci. Geomech. Abstr.* **22,** 85–98.
Maier, G. (1968). Sul comportamento flessionale instabile nelle travi inflesse elasto-plastiche. *Rendiconti Ist Lombardo di Scienze e Lettere, A* **102,** 648–677.
Maier, G., Zavelani, A. and Dotreppe, J. C. (1973). Equilibrium branching due to flexural softening. *J. Engng Mech. ASCE* **99,** 897–901.
Nemat-Nasser, S., Sumi, Y. and Keer, L. M. (1980). Unstable growth of tension cracks in brittle solids. *Int. J. Solids Structures* **16**(11), 1017–1035.
Ottosen, N. S. (1986). Thermodynamic consequences of strain softening in tension. *J. Engng Mech ASCE* **112,** 1151–1164.
Palmer, A. C. and Rice, J. R. (1973). The growth of slip surfaces in the progressive failure of over-consolidated clay. *Proc. R. Soc. Lond.* **A 332,** 527–548.
Salamon, M. D. G. (1970). Stability, instability and design of pillar workings. *Int. J. Rock Mech. Min. Sci.* **7,** 613–631.
Schreyer, H. L. (1990). Analytical solutions for nonlinear strain gradient softening and localization. *J. Appl. Mech.* **112**(3), 522–528.
Schreyer, H. L. and Chen, Z. (1986). One-dimensional softening with localization. *J. Appl. Mech.* **53,** 791–797.
Sture, S. and Ko, H. Y. (1978). Strain-softening of brittle geologic materials. *Int. J. Num. Anal. Mech. Geomech.* **2,** 237–253.
Timoshenko, S. P. and Goodier, J. N. (1970). *Theory of Elasticity* (3rd Edn). McGraw-Hill, New York.
Tognon, G. and Cangiano, S. (1989). Fracture behaviour of high strength and very high strength concretes. *Proc. Int. Workshop on Fracture Toughness and Fracture Energy*, Balkema, Rotterdam, pp. 57–72.
Vardoulakis, I. (1980). Shear band inclination and shear modulus of sand in biaxial tests. *Int. J. Num. Anal. Meth. Geomech.* **4,** 103–119.
Wawersik, W. R. and Fairhurst, C. (1970). A study of brittle rock fracture in laboratory compression experiments. *Int. J. Rock Mech. Min. Sci.* **7,** 561–575.
Wood, R. H. (1968). Some controversial and curious developments in the plastic theory of structures. In *Engineering Plasticity* (Edited by J. Heyman and F. A. Leckie) pp. 665–691. Cambridge University Press, Cambridge, U.K.
Wood, R. H. and Roberts, E. H. (1966). Discussion of A new approach to inelastic structural design by M. G. Lay. *Proc. Inst. Civ. Engng* **35,** 546–549.